SUPPLEMENTAL FIGURE LEGENDS

Suppl. Figure 1. Essential gene inactivations stimulate microbial food aversion and developmental arrest (or delay) phenotypes (relevant to Figure 1; see also Table S1A-C, Movies S1-3).

(A) Aversion phenotypes observed in pilot experiments with growth of animals on RNAi bacteria inactivating essential *C. elegans* genes. Aversion behavior required RNAi-proficiency, and was abolished in two RNAi defective *C. elegans* mutants, *sid-1(qt9)* and *rde-1(ne219),* in response to *tars-1* RNAi. A key containing brief functional descriptions for each essential gene inactivation is shown to the right of the graph. Statistical analyses: *** indicates $p<0.001$ for pair-wise comparisons using the student's t-test. Comparisons made were between a gene inactivation and the RNAi control (harboring an empty dsRNA vector), or between wild type and RNAi-defective mutant animals in response to *tars-1* RNAi.

(B) Microbial aversion is a phenotype that develops over time. Hatchlings were plated to RNAi lawns of uniform size and density and were assayed for aversion frequency at multiple time points during development. Aversion behavior was unobservable in the first 24 hours of the experiment, but became evident by ~40 hrs of growth, and continued to increase through the termination of the experiment at 56hr. Statistical analyses were performed at the 56 hour time point: ** indicates $p<0.001$, *** indicates $p<0.0001$. RNAi of the essential gene *cdk-1* (encoding a cyclin-dependent kinase) did not stimulate aversion and was indistinguishable from the RNAi control phenotypically.

(C) A time course showing basal aversion rates for animals grown on the RNAi control strain. Aversion was undetectable during the first three larval stages (L1, L2 and L3), became barely detectable in the 4th larval stage (L4) at ~45 hrs, and started to rise as animals matured into reproductive adults at ~48 hrs. Because it seemed optimal for detection of aversion phenotypes while keeping background levels of aversion low, the 48-58 hour frame was selected as the interval during which aversion would be measured in the RNAi screen of essential genes displayed in Figure 1C,D and Table S1A.

(D) Comparison of developmental phenotypes in aversion gene set relative to the set of essential and metabolic genes surveyed. While only 19% of the set of genes screened produced a larval developmental arrest or delay, 85% of the aversion gene set produced arrest or delayed development. For ease of description in the text, we've referred to the developmental "arrest" phenotypes resulting from essential gene RNAi treatments. However - because we did not generally continue to monitor the developmental progress of RNAi-treated animals beyond the 58hr time point, we can not establish with certainty which developmental phenotypes represent true arrests and which represent a general slowing of development that may ultimately culminate in adult maturity. Some arrests/delays produced animal of uniform stage; others produced a heterogeneous developmental population (See Table S1A).

(E) An area-proportional set diagram of overlap between aversion and developmental phenotypes observed in the first 58hr of RNAi exposure. The majority of aversion phenotypes were coincident with developmental arrest or delay, while many developmental phenotypes (~62%) were not accompanied by detectable aversion phenotypes.

Suppl. Figure 2. Stimulation of pathogen-associated, detoxification and other transcriptional stress responses by essential gene inactivations (relevant to Figure 3; see also Table S2).

(A) The hypodermal *nlp-29::GFP* reporter (induced by *D. coniospora* or wounding to the cuticle) is stimulated by inactivation of *pan-1* (a leucine-rich transmembrane protein), and the *nhr-23* and *nhr-25* nuclear hormone receptors, all genes required for execution of the molting program and

hypodermal maintenance. Although some overlap was observed, the RNAi-mediated induction pattern of *nlp-29::GFP* was largely distinct from the three pathogen-induced reporters examined in Figure 3A. See Table S2A for a complete list of gene inactivations that stimulated the *nlp-29::GFP* reporter.

(B) Other transcriptional stress reporters were stimulated by essential gene inactivations. *gpdh-1::GFP*, *hsp-4::GFP*, *hsp-6::GFP* and *sod-3::GFP* are characterized reporters for induction of osmotic, ER, mitochondrial and oxidative stress responses, respectively. Aversion-inducing gene inactivations produced frequent stimulation of these stress response pathways in addition to pathogen and detoxification reporters. Shown: induction of *gpdh-1::GFP* by inactivation of *osm-11* (required for osmotic shock responses) and *tars-1* (a tRNA synthetase); induction of *hsp-4::GFP* by inactivation of *tkt-1* (transketolase) and *vha-3* (a vacuolar ATPase subunit); induction of *hsp-6::GFP* by inactivation of *atp-2* (an ATP synthase subunit) or *vha-3*; induction of *sod-3::GFP* by inactivation of *tkt-1* and *rpl-1* (a large ribosomal subunit). See Table S2B for full list of reporter inductions.

(C) Summary and enrichment table for pathogen-associated, detoxification and general cellular stress responses induced by aversion-inducing gene inactivations. Frequencies of activation of all reporters examined in Figure 3 and above in comparison to frequencies of reporter induction by a random gene set derived from the first two 96-well plates of the whole genome RNAi library. Depending on the reporter examined, there was anywhere between a 2-fold and 35-fold enrichment for reporter activation. The level of enrichment for the *hsp-4::GFP* reporter was not possible to determine because none of the randomly selected RNAi clones were found to induce it. Statistical significance was assessed by chi-squared test ($p<0.0001$ for all comparisons between the aversion gene subset and the random set tested for a given reporter).

Suppl. Figure 3. Validation and testing of tissue-restricted RNAi strains (relevant to Figure 4; See also Figure S4, Table S3).

(A) Images showing the normal expression pattern of the systemically expressed *sur-5pr::GFP^{NLS}* transgenic strain used to assess the fidelity of intestine and hypodermis-restricted RNAi strains. Hypodermal, intestine (gut), head neuron and pharyngeal nuclei are all readily visible (labeled) when animals were raised on the RNAi control strain.

(B) Images of gut and hypodermal silencing of GFP when *sur-5::GFP^{NLS}* animals were raised on *E. coli* expressing dsRNA targeting the *gfp* gene. GFP is still visible in head neurons, pharyngeal cells and the nerve cord because these tissues are refractory to RNAi.

(C) Intestine-specific silencing of GFP in the *sid-1(qt9); Is[vha-6pr::sid-1]; Is[sur-5pr::GFP^{NLS}]* strain in response to GFP RNAi feeding. This strain is RNAi defective in all tissues due to the *sid-1(qt9)* mutation, but wild type *sid-1* is restored to the intestine by fusion of the *sid-1* coding sequence to the *vha-6* intestine-specific promoter. Three focal planes are shown, moving from the bottom focal plane (the side abutting the glass slide), through the gut layer in the middle focal plane and up to the top focal plane (closest to the microscope lens). Hypodermal nuclei are easily seen in the "bottom" and "top" focal planes but the large intestinal nuclei that appear so prominently in control RNAi animals are no longer visible, indicating that GFP expression has been silenced in this tissue. A hazy (and characteristic) background gut fluorescence is visible in the middle focal plane, indicating that this is the correct plane to view gut nuclei if the *sur-5pr::GFP^{NLS}* transgene were still undergoing expression in this tissue. In contrast, hypodermal nuclei, muscle nuclei, the nerve cord, head and pharyngeal nuclei are still GFP-labeled, indicating that GFP is not silenced in these tissues.

(D) Hypodermis-specific silencing of GFP in the *rde-1(ne219); Is[wrt-2pr::rde-1]; Is[sur-5pr::GFP^{NLS}]* in response to *gfp* RNAi. In the multiple focal planes represented in this sample, there is

no evidence of hypodermal GFP expression, while GFP expression is observed in the intestine, muscle, pharynx, neurons and nerve cord. A DIC image showing the hypodermal layer (identifiable by the characteristic longitudinal alae structure) with a paired focal plane image viewed in the GFP fluorescence channel confirmed that GFP expression is abolished in hypodermal cells but not the other major cell types in this strain.

For all samples (A-D), animals were visualized at 48-58 hrs of *gfp* feeding, the same time interval used to score aversion phenotypes, ensuring that tissue-specific gene silencing takes place in the necessary time frame.

Suppl. Figure 4. Gene inactivations restricted to the hypodermis or intestine stimulate aversion behavior (related to Figure 4; see also Table S3)

(A) Inactivation of known intestine-specific genes, *elt-2* and *pept-1*, in the intestine-restricted but not the hypodermis-restricted RNAi strain stimulated microbial aversion, confirming the absence of "leaky" intestinal expression of the rescuing RNAi transgene in the hypodermis-restricted RNAi strain.

(B) Inactivation of two genes with characterized hypodermal functions but no known intestinal functions, *qua-1* and *lin-41*, in the hypodermis-restricted but not the intestine-restricted RNAi strain stimulated microbial aversion, confirming the absence of "leaky" hypodermal expression of the rescuing RNAi transgene in the intestine-restricted RNAi strain.

(C-D) Inactivation of different protein translation components in the hypodermis-restricted or intestine-restricted RNAi lines yielded a curious discrepancy. (C) When ribosomal components (represented by *rpa-0* and *rpl-41*) or a tRNA synthetase (*tars-1*) were inactivated in the hypodermis, aversion behavior was stimulated. (D) When ribosomal components (*rpl-1* or *rpl-41*) were inactivated in the intestine-restricted RNAi strain, aversion behavior was also stimulated. However, inactivation of neither the *tars-1* nor *cars-1* tRNA synthetase genes (encoding threonyl and cysteinyl tRNA synthetases, respectively) stimulated aversion behavior in the intestine-restricted RNAi strain.

Suppl. Figure 5. Analysis of aversion behavior control by known pathogen and stress response signaling pathways (relevant to Figure 5.)

(A) Left panel: Basal aversion levels of Jnk pathway mutants are low and similar to wild type animals. Middle and Right panels: *kgb-1(km21)* mutants exhibit partial suppression of aversion behavior induced by inactivation of tRNA synthetase genes (*tars-1* or *kars-1*) or vacuolar ATPase subunit genes (*vha-6* and *vha-12*), while *mek-1* and *mlk-1* mutants still exhibit strong suppression of the behavior.

(B) The p38-like MAP kinase cascade is not required for aversion behavior. For most gene inactivations tested, *nsy-1*, *sek-1* and *pmk-1* mutations did not have a significant effect on aversion behavior. Examination of two mutant alleles in *tir-1*, encoding a Toll-related receptor and additional alleles of *nsy-1* and *pmk-1* have confirmed this result across all functional classes of gene inactivation tested (data not shown). However, *sek-1(qd39)* (shown) and *sek-1(qd4*) (not shown) mutants exhibited a partial defect in response to inactivation of tRNA synthetases (*tars-1* and *kars-1*), vacuolar ATPAse subunits (*vha-6* and *vha-12*), and ATP synthase subunits (*atp-2* and *atp-4*) but not other types of gene inactivations (proteasome components, other protein translation and mitochondrial components).

(C) Analysis of *fshr-1* and *zip-2* pathogen defense pathways showed that these genes do not contribute to the aversion response. Interpretation of *fshr-1(ok778)* data were complicated by a high basal aversion rate on RNAi control bacteria. However the RNAi clones tested also caused larval

arrest, and are more properly compared to stage-matched controls, which generally exhibit low or undetectable aversion phenotypes. We did not conduct a developmental time course with *fshr-1*, so we cannot formally rule out the possibility that although *fshr-1* itself exhibits a high aversion rate, it might also suppress the aversion induced by noxious RNAi treatments.

Suppl. Figure 6. The function of learning and neurosensation in control of aversion behavior (relevant to Figure 6).

(A) RNAi targeting *nhx-2*, *kars-1*, *atp-2* or *hsp-60* genes caused larval arrest or retarded entry into adulthood. Shown are representative examples drawn from the same populations of animals used in the associative learning assays presented in Figure 6B. Animals were examined for evidence of recovery from developmental arrest after 2 days on tester plates (28 hrs after the final time point (20hr) for scoring aversion behavior. All images have been magnified 40x. For the purpose of size and stage comparison, shown at right are wild type animals grown continuously on empty vector control bacteria (HT115) and *sid-1(qt9)* mutant animals defective for RNAi grown continuously on noxious *kars-1* RNAi bacteria. Both controls have been reproductively mature adults for 2 days.

(B) Animals were examined for behavioral aversion in response to *kars-1* RNAi when transferred to test plates containing bacterial lawns of different microbial species. The species tested *B. subtilis*, *B. simplex* and a *Comamonas* species are known residents of soil and decomposing environments and may represent more ecologically relevant food options for *C. elegans*. However, the results of this experiment mirrored those shown in Figure 6B: animals showed similar levels of microbial avoidance at early time points but by 14 and 22 hours avoided the HT115 strain at significantly higher frequencies than the non-HT115 strains regardless of species type (*** indicates $p<0.001$).

(C) Developmental time course showing basal aversion frequencies of neurosensory mutants on RNAi control bacteria. By adulthood (48 hr), *che-2(e1033)* and *che-3(e1124)* mutants showed elevated basal aversion to benign *E. coli* ($p<0.01$ by students t-test). Other sensory mutants may exhibit slightly elevated aversion relative to wild type animals, although these effects were not statistically discernible.

(D-G) Mutants in chemosensation (*che-2(e1033)* and *che-3(e1124)*), mechanosensation (*mec-3(e1338)*, *mec-4(u45)*, and *mec-7(e1527)*), thermotaxis (*ttx-1(p767)* and *ttx-4(nj3)*), aerotaxis/hyperoxia avoidance (*gcy-35(ok769)*) were evaluated for their ability to avoid *E. coli* in response to essential gene inactivations. A *tax-4(p678)* mutant, defective for multiple sensory modalities, was also tested. Essential gene inactivated tested were: *vha-6* (a vacuolar ATPase subunit), *kars-1* (a tRNA synthetase), *cco-1* (cytochrome c oxidase, an electron transport chain component) and *elt-2* (a GATA transcription factor required for gut development). Because neurosensory mutants showed some basal elevation of aversion level on control RNAi bacteria, aversion was evaluated and plotted in two forms for each mutant: (1) in raw form (the unadjusted aversion frequency – i.e. the fraction of total animals found off the lawn) and (2) in background-normalized form, where the levels of aversion on RNAi control lawns had been subtracted from the raw aversion score. Of all mutants tested, only the *tax-4* mutant was defective in eliciting an aversion response to all four essential gene inactivations. The *che-2* and *che-3* chemosensory mutants were defective in response to two of the four gene inactivations tested (*cco-1* and *elt-2*). The mechanosensory, thermotaxis and aerotaxis mutants tested showed no deficit in any of these assays.

Suppl. Figure 7. Sensory responsiveness of animals in a microbial aversion state induced by essential gene inactivations (relevant to Figure 6).

(A) Pharyngeal pumping rates have been shown to decrease in response to some microbial pathogens or low nutritive value of a microbial food source. We examined the pharyngeal pumping rates of animals raised on 10 different gene inactivations. Because little is known of the pharyngeal pumping rates of juvenile animals and our experimental samples needed to be stage-matched with control samples, we selected for analysis only those gene inactivations that produced gravid (egg-producing) adults (with the exception of *kars-1* RNAi, which produces L4 stage and sterile adults). A list of the genes selected and brief functional descriptions are provided to the right of the graph. Pharyngeal pumping was measured for 45-60 seconds in a minimum of 30 animals over 2-3 independent trials. Results were averaged across trials. Statistical significance was determined by students t-test followed by Bonferroni correction for multiple comparisons (*$p<0.01$, **$p< 0.001$ and ***$p<0.000001$). Although the effects were modest for most RNAi treatments, a statistically significant reduction in pumping rates were observed in nine of ten cases. Inactivation of *ftt-2* (which encodes a 14-3-3 protein) produced the most profound reduction in pumping (35 pumps/min compared to 332 pumps/min in the RNAi control.)

(B-E) Animals were tested for their ability to respond to positive and negative olfactory, gustatory and mechanosensory cues following treatment with essential gene RNAi. Olfactory attraction behavior was assessed by evaluating chemotaxis efficiency when animals were exposed to the volatile odorant isoamyl alcohol (B). Gustatory attraction was tested by measuring chemotaxis to the soluble attractant NH_4Cl (C). Olfactory avoidance was measured in response to the noxious volatile odorant, octanol. (D). Mechanosensory defenses were measured by scoring reversal frequency in response to gentle body touch (E). See Supplemental Experimental Procedures for a detailed description of each assay. Statistical significance was determined using the students t-test (*$p<0.01$, ***$p<0.0001$).

SUPPLEMENTAL TABLE LEGENDS

Suppl. Table 1. RNAi screen for aversion behavior (related to Figure 1).

(A) Gene inactivations that stimulated microbial aversion behavior in a screen of 4,062 essential and metabolic genes. Presented according to functional category, the list of 379 gene inactivations that induced microbial aversion after 48-56hr growth on RNAi *E. coli*. Shown are Sequence and Gene names, mean aversion values and standard errors, animal developmental stage at time of scoring (L1->L4 represent the four larval stages, SA = sterile adult, GA = gravid adult), # of independent replicates (with 3 trials per replicate), and a brief description of gene identity/function according to WormBase annotations retrieved using WormMart.

(**B) Aversion-inducing genes exhibit elevated conservation with the human proteome.** Comparison of protein conservation between *C. elegans* and *H. sapiens* for a) the 379 aversion genes, b) the 4,062 essential and metabolic genes screened, and c) the whole *C. elegans* proteome. Shown are the number/percentage of genes from each group when parsed into one of eleven bins corresponding to increasing degrees of protein identity (0->100%). Average *C. elegans*/*H. sapiens* protein conservation for each gene group is displayed at bottom.

(C) Aversion genes associated with human disorders. Twenty-two genes identified in the aversion screen cause human disease when mutated.

Suppl. Table 2. Summary data for innate immune, detoxification and stress reporter induction (related to Figure 3).

(A) Innate immune/pathogen-associated and drug detoxification reporters induced in

response to inactivation of a subset of aversion genes representing the major functional classes identified in the aversion screen. Data are displayed in "heat map" format, where darker shades (green for innate immune reporters, purple for drug detoxification reporters) indicate qualitative degree of induction based on visual examination over multiple replicates. Column heading key indicates identity of each reporter analyzed.

(B) Activation of other reporters of cellular stress in response to essential gene inactivations. As in (A), induction of reporters for mitochondrial stress, ER stress, osmotic stress and oxidative stress shown in "heat map" format, with dark blue indicating strongest induction.

Suppl. Table 3. List of aversion-associated genes with expression patterns that exclude the nervous system (related to Figure 4).

At least 26 genes identified in the aversion screen are not expressed in neurons, suggesting that aversion behavior is a product of endocrine communication between neuronal and non-neuronal tissues. The genes on this list are expressed in one or more of the following tissues: the intestine, hypodermis, germline, pharynx, vulva, body wall muscle and the excretory cell, suggesting that each of these tissues may be competent to induce aversion behavior when in distress. *vha-8* is only expressed in the excretory cell, suggesting that disruption of cellular processes in only a single cell may be sufficient to engage the aversion response. Primary references for each gene expression pattern are provided.

Suppl. Table 4. *C. elegans* and microbial strains used in this study (related to Experimental Procedures).

SUPPLEMENTAL MOVIE LEGENDS

Movie S1. Control (-) RNAi animals rarely leave the bacterial lawn (related to Figure 1.)

Playback speed for all movies is accelerated 40x relative to real time. Animals were filmed at 5X magnification on lawns of fixed shape, density and size after 48-56hr of growth on RNAi or control RNAi lawns.

Movie S2. Lawn aversion behavior in calcineurin RNAi-treated animals (related to Figure 1.)

Aversion behavior was induced by inactivation of *Y71H2AL.1*, the *C. elegans* homolog of calcineurin B.

Movie S3. Lawn aversion behavior in *atp-2* RNAi-treated animals (related to Figure 1.)

Aversion behavior was induced by inactivation of *atp-2*, an ATP synthase subunit. Animals in this movie are significantly smaller than in the RNAi control due to developmental arrest at ~L3 larval stage.

SUPPLEMENTAL EXPERIMENTAL PROCEDURES

Detailed descriptions of experimental procedures used in this study can be found below.

RNAi avoidance assays

RNAi bacterial clones were picked or stamped in 96-well format from -80°C glycerol stocks to rectangular LB/Tet/Amp plates and grown at 37°C o/n prior to amplification in culture. Rectangular plates could be kept at 4°C for up to 2-3 weeks prior to experimental use. More extended 4°C storage can lead to loss of efficacy for some clones. Bacteria were inoculated into 7 mls liquid volume LB/carbenicillin (50ug/ml) in 10ml x 24-well rectangular plates (Promega Cat# V6831 or Dot Scientific Cat# SC74324-NS7), sealed with Breathe-Easy strips (USA Scientific Cat# 9123-6100), and grown in a 37°C shaker to near saturation (20-24hr). Bacteria were pelleted and resuspended in 150 ul 30-40X LB/carb. Three 50ul aliquots per RNAi clone were dropped to the center of each well on 6-well RNAi plates, taking care not to splatter bacteria, puncture agar surface, or agitate wet bacteria and dried. Only circular lawns of uniform size and density (approximate) were used for aversion assays. Dried plates were kept at RT for 16-24hr prior to experiment to allow IPTG induction of dsRNA. On the day prior to setting up overnight RNAi cultures, animals (2,000-3,000) were chunked or washed from freshly starved plates (L1/L2s) to 10ml NGM plates containing 20X concentrated HB101 and grown on bench top (23-24°C) for 2dy or until gravid adults, harvested for embryos by hypochlorite treatment (Hope, 1999), and hatched overnight (~12-16hr) in S Basal. Egg preps should be performed on the same day as RNAi assay plate preparation. On the following day, synchronized hatchlings (~60 animals in 5-15 ul liquid volume) were serially aliquoted to the center of each bacterial lawn using a repeat pipettor. Aversion assays were typically scored at 48-58hr (on bench top at 23-24°C), although occasionally animals were incubated with RNAi for up to 64 hr before robust aversion. Control RNAi plates become unreliable >56-58hr due to depletion of bacteria and loss of distinct lawn boundary caused by animal locomotion. Animals were scored for aversion using a Nikon SMZ800 microscope. The number of animals located off the RNAi lawn (N_{off}) and the total number of animals per well (N_{total}) were counted. For the RNAi screen, wells were visually inspected prior to counting, and only samples appearing to be aversion candidates were scored. Aversion = N_{off}/N_{total} and was averaged across 3 replicates. Positives were confirmed by independent replicates (usually>3) and sequence-verification of the RNAi clone. Approximate developmental stage was recorded for all RNAi clones tested.

Toxin avoidance assays

OP50 cultures were grown at 37°C and concentrated 10-20X in S Basal. Aliquots (50ul) of concentrated OP50 were dropped to 6-well NGM assay plates similar to above; 250-350 ul were dropped to pre-assay growth plates. Synchronized L1s were reared on OP50 growth plates until the desired developmental stage (we tested drug responses in both L3 and L4/adult stage animals), washed in S Basal and transferred to assay lawns containing toxin or solvent control. Assay plates were prepared by adding solvent +/- drug directly to the OP50 lawn ~1hr prior to beginning an experiment. For initial experiments, a drug dilution series was used, and aversion was measured in 2 hr increments for the first 12 hours, concluding with terminal time points as late as 24hr. All assays were performed in triplicate and were independently replicated $\geq$3 times, usually with 2-3 different drug concentrations, as drug potency seemed somewhat variable between days. Most drugs are not water soluble, and in organic solvents they precipitate to varying degrees once dropped to bacterial lawns. DMSO was usually the most effective solvent, but it was also the most likely to produce black

precipitates upon plating. Though drugs were less soluble in EtOH and MeOH than in DMSO, precipitation upon plating was less of a problem, so these solvents were used wherever possible. Solvents often had weak aversion effects on their own, so minimal solvent volumes were used to achieve effective doses of drug. All drug treatments required same-volume solvent controls.

Drugs, solvents, peak time points, and final drug concentrations (calculated according to total agar volume) used in lawn aversion experiments:
Antimycin A (EtOH, 4-8hr): 25 ug/ml
Bortezomib (DMSO, 6-8hr): 60 ug/ml
Concanamycin A (MeOH, 8-12hr): 500 ng/ml
Geneticin (water, 3-6hr): 250 ug/ml
Paraquat (water, 6-8hr): 250 ug/ml
Tunicamycin (MeOH, 24hr): 50 ug/ml
Zeocin* (water, 10-16hr): 400 ug/ml

*Zeocin is salt-labile and is rapidly inactivated on NGM plates. Maximal induction of aversion was achieved by ~30-60min pre-incubation of worms with Zeocin in 0.5X S Basal or HBSS low salt buffer prior to addition of animals to Zeocin-supplemented OP50 lawns.

GFP reporter experiments
Transgenic strains for visualization of innate immunity, detoxification and stress responses carried integrated high-copy arrays containing the promoter elements of genes of interest fused to GFP. Full genotypes, strain sources and original publications describing use of each strain are provided in the Supplemental Strain Table. For reporter induction experiments, ~30-50 animals were serially aliquoted to 12 or 24-well RNAi plates that had been seeded with 200-300ul unconcentrated o/n RNAi cultures and dried 3-4hr in hood on previous day. RNAi plates were either grown at RT (23-24°C) for 2dy or 20°C for 3dy prior to scoring (after confirming reproducibility of results between growth conditions.) Each RNAi clone was tested in duplicate on a given day, and results were reproduced in 2-3 independent replicates.

Imaging
A Zeiss Axioplan2 fluorescent compound microscope connected to a Hamamatsu ORCA-ER black & white camera and camera controller and a MacIntosh computer equipped with OpenLab5.0.1 imaging software was used to collect images for the following transgenes: *F35E12.5::GFP*, *irg-1::GFP*, *clec-60::GFP*, *cyp-35B1::GFP*, *nlp-29::GFP*, *sur-5::GFP*^{NLS}, *sur-5::GFP*^{NLS}, *sid-1(qt9)*; *vha-6::sid-1*; *sur-5::GFP*^{NLS}, and *rde-1(ne219); vha-6::rde-1; sur-5::GFP*^{NLS}. GFP and DIC images were captured at 16X magnification (16X/40X for tissue-specific lines) using fixed exposure settings. False color was applied to pathogen and detoxification reporter images.

A Zeiss Discovery.V12 Stereo Microscope connected to a Zeiss Axiocam HSc color camera and Dell computer equipped with Zeiss Axiovision 4.5 imaging software was used to collect GFP fluorescent images of animals on worm plates for gst-4::GFP, sod-3::GFP, gpdh-1::GFP, hsp-6::GFP transgenic lines, and for figures showing lawn aversion behavior.

Tissue-restricted RNAi experiments
Construction of hypodermis and intestine-specific RNAi strains:

Hypodermis-restricted RNAi (constructed/validated in collaboration with John Kim and Vishal Khivanasara): A *wrt-2* promoter fragment shown to drive expression in the syncytial hypodermis and seam cells was fused to a full-length genomic fragment encoding *rde-1*. The *wrt-2::RDE-1* construct was injected into *rde-1(ne219)* mutant animals with a *myo2::RFP3* selection marker and pBluescript carrier to a final DNA concentration of 100 ng/ul. The extrachromasomal array was integrated by UV irradiation and tested for tissue-specificity of rescue (below and shown in Figure S3). Once validated for specificity, the *wrt-2::RDE-1* line was subsequently backcrossed 10X to N2 and re-crossed into *rde-1(ne219)* for use in hypodermally-restricted RNAi experiments.

Intestine-restricted RNAi (constructed/validated in collaboration with Alex Soukas): a *sid-1* genomic fragment was fused to a 900 bp fragment of the *vha-6* promoter shown to confer intestinally-restricted expression (H.Y. Mak and E. O'Rourke, personal communication) and a synthetic intron, and preceding coding sequences for SL2-GFP (providing co-expression of GFP under the same *vha-6* promoter).

Validation of tissue-restricted RNAi activity:

To confirm the accuracy of tissue-restricted RNAi lines, a *sur-5::SUR-5-GFP*^{NLS} integrated transgene (expressed systemically throughout the soma) was crossed into the each of the rescued RNAi strains (restoring RNAi to hypodermis or intestine). Animals were fed dsRNA corresponding to GFP and examined for GFP expression in major bodily tissues (hypodermis, muscle, neurons, and intestine.) If GFP expression was eliminated in the desired tissue without disruption of GFP expression in other tissues, the strain was used for tissue-restricted RNAi experiments. Images of tissue-restricted GFP silencing and additional functional validation are shown in Suppl. Figure 3.

Associative learning assays

Synchronized wild type (N2) or *sid-1(qt9)* hatchlings were reared for ~54hr on growth plates containing control or noxious RNAi bacteria. Animals were washed from growth plates, then washed 2-3x in S Basal prior to transfer to test plates. Test plates were prepared as described above, and animals were transferred to one of four 6 cm assay plates containing control RNAi (HT115), noxious RNAi (HT115 with a dsRNA targeting an essential *C. elegans* gene), HB101 or OP50 *E. coli*. Aversion was measured at the intervals specified in text. Learning assays presented in Figure S5 included additional bacterial species: *B. subtilis*, *B. simplex* and *Comamonas*.

Chemotaxis assays

Chemotaxis assays for volatile and soluble attractants and repellents were performed and the data were analyzed essentially as described in (Hart, 2006) and (Bargmann et al., 1993). Synchronized L1s were grown on aversion-inducing RNAi bacteria or control RNAi bacteria for 48-54 hr prior to conducting behavioral assays. Animals were tested for attraction to a spot of 1 ul isoamyl alcohol on fresh 10cm NGM plates. Animals were tested for attraction to 20 mM NH_4Cl by a quadrant assay on freshly poured 2% agar 5mM KPO_4 buffered 10cm 4-quadrant Petri plates (VWR Cat#25384-308) after washing 3X with CTX buffer. Assays of repulsion to undiluted 1-octanol were performed on fresh NGM in 6 cm square plates. Chemotaxis was measured after one hour and calculated using the standard formula (CI= (# of animals on odorant-# of animals on control)/(total number of animals)). All assays were performed in triplicate in at least 3 independent trials. Approximately 50-100 animals were tested per assay plate.

Mechanosensation assay

Animals were tested for touch avoidance after 48-54 hrs of growth on RNAi or control bacteria. Touch avoidance was measured directly on growth plates by performing 6 alternating light taps to the head or tail, and counting the number of times a tap resulted in locomotory reversal of 2 or more body bends. At least 20 animals were tested in at least 3 independent trials for each RNAi treatment.

Pharyngeal pumping assays

Animals were raised on RNAi or control bacteria for 50-60hr prior to measurement of feeding rates. With the exception of *kars-1* RNAi treated animals (which were L4/sterile adults) only gravid adults were assayed for pumping to ensure so all samples would be stage-matched with the RNAi control. (The influence of developmental stage on pharyngeal pumping rates is unknown.) Individual animals were filmed for a minimum of 60 seconds each using a Sony video camera mounted on a Zeiss M2 microscope. Apple iMovie was used for video recording and analysis. RNAi control animals were filmed at the beginning and end of each experiment to ensure that room conditions were stable through the experiment. Movies were subsequently examined at 25-50% replay speed in order to accurately count pharyngeal contractions. The number of contractions over intervals of 40-60 sec was counted for each animal and have been reported as pharyngeal contractions/min. At least 10 animals were tested per RNAi treatment within an experiment, and results were averaged in 2 independent trials.

Statistical Methods

The student's t-test and chi-squared tests were used to validate behavioral results as stated in figure legends. Bonferroni correction for multiple comparisons was applied to p-value calculations in learning and pharyngeal pumping assays. Multiple comparison adjustments were not performed if results were independently verified with multiple alleles or gene inactivations, and the p-values were sufficiently low ($p<0.01$). Standard error of the mean (SEM) was reported for all aversion-inducing RNAi clones in Table S1. DAVID enrichment analysis provided statistical significance for functional categories identified in the screen, and p-values from DAVID analysis were Benjamini method-corrected for multiple comparisons. For more information about the DAVID tool, visit: http://david.abcc.ncifcrf.gov/home.jsp.

Statistical Notes on Figures 4B-D, 5B-D, 6C, S4A-D, S5A-B:

P-values were generated by student's t-test from pooled data for each functional class in an experiment.

SUPPLEMENTAL REFERENCES

References associated with Table S3: Aversion-associated genes with extra-neuronal post-embryonic expression patterns.

Asahina, M., Ishihara, T., Jindra, M., Kohara, Y., Katsura, I., and Hirose, S. (2000). The conserved nuclear receptor Ftz-F1 is required for embryogenesis, moulting and reproduction in Caenorhabditis elegans. Genes Cells *5*, 711-723.

Boag, P.R., Nakamura, A., and Blackwell, T.K. (2005). A conserved RNA-protein complex component involved in physiological germline apoptosis regulation in C. elegans. Development *132*, 4975-4986.

Brock, T.J., Browse, J., and Watts, J.L. (2006). Genetic regulation of unsaturated fatty acid composition in C. elegans. PLoS Genet *2*, e108.

Calfon, M., Zeng, H., Urano, F., Till, J.H., Hubbard, S.R., Harding, H.P., Clark, S.G., and Ron, D. (2002). IRE1 couples endoplasmic reticulum load to secretory capacity by processing the XBP-1 mRNA. Nature *415*, 92-96.

Chen, Z., Eastburn, D.J., and Han, M. (2004). The Caenorhabditis elegans nuclear receptor gene nhr-25 regulates epidermal cell development. Mol Cell Biol *24*, 7345-7358.

Choi, K.Y., Ji, Y.J., Dhakal, B.K., Yu, J.R., Cho, C., Song, W.K., and Ahnn, J. (2003). Vacuolar-type H+-ATPase E subunit is required for embryogenesis and yolk transfer in Caenorhabditis elegans. Gene *311*, 13-23.

Fisher, A.L., Page, K.E., Lithgow, G.J., and Nash, L. (2008). The Caenorhabditis elegans K10C2.4 gene encodes a member of the fumarylacetoacetate hydrolase family: a Caenorhabditis elegans model of type I tyrosinemia. J Biol Chem *283*, 9127-9135.

Frand, A.R., Russel, S., and Ruvkun, G. (2005). Functional genomic analysis of C. elegans molting. PLoS Biol *3*, e312.

Fukushige, T., Goszczynski, B., Yan, J., and McGhee, J.D. (2005). Transcriptional control and patterning of the pho-1 gene, an essential acid phosphatase expressed in the C. elegans intestine. Dev Biol *279*, 446-461.

Fukushige, T., Hawkins, M.G., and McGhee, J.D. (1998). The GATA-factor elt-2 is essential for formation of the Caenorhabditis elegans intestine. Dev Biol *198*, 286-302.

Hunt-Newbury, R., Viveiros, R., Johnsen, R., Mah, A., Anastas, D., Fang, L., Halfnight, E., Lee, D., Lin, J., Lorch, A*., et al.* (2007). High-throughput in vivo analysis of gene expression in Caenorhabditis elegans. PLoS Biol *5*, e237.

Iwasaki, K., McCarter, J., Francis, R., and Schedl, T. (1996). emo-1, a Caenorhabditis elegans Sec61p gamma homologue, is required for oocyte development and ovulation. J Cell Biol *134*, 699-714.

Ji, Y.J., Choi, K.Y., Song, H.O., Park, B.J., Yu, J.R., Kagawa, H., Song, W.K., and Ahnn, J. (2006). VHA-8, the E subunit of V-ATPase, is essential for pH homeostasis and larval development in C. elegans. FEBS Lett *580*, 3161-3166.

Jones, A.R., Francis, R., and Schedl, T. (1996). GLD-1, a cytoplasmic protein essential for oocyte differentiation, shows stage- and sex-specific expression during Caenorhabditis elegans germline development. Dev Biol *180*, 165-183.

Kawasaki, I., Hanazawa, M., Gengyo-Ando, K., Mitani, S., Maruyama, I., and Iino, Y. (2007). ASB-1, a germline-specific isoform of mitochondrial ATP synthase b subunit, is required to maintain the rate of germline development in Caenorhabditis elegans. Mech Dev *124*, 237-251.

Komatsu, H., Chao, M.Y., Larkins-Ford, J., Corkins, M.E., Somers, G.A., Tucey, T., Dionne, H.M., White, J.Q., Wani, K., Boxem, M.*, et al.* (2008). OSM-11 facilitates LIN-12 Notch signaling during Caenorhabditis elegans vulval development. PLoS Biol *6*, e196.
Kontani, K., Moskowitz, I.P., and Rothman, J.H. (2005). Repression of cell-cell fusion by components of the C. elegans vacuolar ATPase complex. Dev Cell *8*, 787-794.
Kostrouchova, M., Krause, M., Kostrouch, Z., and Rall, J.E. (1998). CHR3: a Caenorhabditis elegans orphan nuclear hormone receptor required for proper epidermal development and molting. Development *125*, 1617-1626.
Kuervers, L.M., Jones, C.L., O'Neil, N.J., and Baillie, D.L. (2003). The sterol modifying enzyme LET-767 is essential for growth, reproduction and development in Caenorhabditis elegans. Mol Genet Genomics *270*, 121-131.
Kuwabara, P.E., Lee, M.H., Schedl, T., and Jefferis, G.S. (2000). A C. elegans patched gene, ptc-1, functions in germ-line cytokinesis. Genes Dev *14*, 1933-1944.
Li, Y., and Paik, Y.K. (2011). A potential role for fatty acid biosynthesis genes during molting and cuticle formation in Caenorhabditis elegans. BMB Rep *44*, 285-290.
MacQueen, A.J., Baggett, J.J., Perumov, N., Bauer, R.A., Januszewski, T., Schriefer, L., and Waddle, J.A. (2005). ACT-5 is an essential Caenorhabditis elegans actin required for intestinal microvilli formation. Mol Biol Cell *16*, 3247-3259.
Mahoney, T.R., Luo, S., Round, E.K., Brauner, M., Gottschalk, A., Thomas, J.H., and Nonet, M.L. (2008). Intestinal signaling to GABAergic neurons regulates a rhythmic behavior in Caenorhabditis elegans. Proc Natl Acad Sci U S A *105*, 16350-16355.
Nehrke, K. (2003). A reduction in intestinal cell pHi due to loss of the Caenorhabditis elegans Na+/H+ exchanger NHX-2 increases life span. J Biol Chem *278*, 44657-44666.
Nehrke, K., and Melvin, J.E. (2002). The NHX family of Na+-H+ exchangers in Caenorhabditis elegans. J Biol Chem *277*, 29036-29044.
Oka, T., Yamamoto, R., and Futai, M. (1997). Three vha genes encode proteolipids of Caenorhabditis elegans vacuolar-type ATPase. Gene structures and preferential expression in an H-shaped excretory cell and rectal cells. J Biol Chem *272*, 24387-24392.
Oka, T., Yamamoto, R., and Futai, M. (1998). Multiple genes for vacuolar-type ATPase proteolipids in Caenorhabditis elegans. A new gene, vha-3, has a distinct cell-specific distribution. J Biol Chem *273*, 22570-22576.
Ono, K., Parast, M., Alberico, C., Benian, G.M., and Ono, S. (2003). Specific requirement for two ADF/cofilin isoforms in distinct actin-dependent processes in Caenorhabditis elegans. J Cell Sci *116*, 2073-2085.
Pujol, N., Bonnerot, C., Ewbank, J.J., Kohara, Y., and Thierry-Mieg, D. (2001). The Caenorhabditis elegans unc-32 gene encodes alternative forms of a vacuolar ATPase a subunit. J Biol Chem *276*, 11913-11921.
Reese, K.J., Dunn, M.A., Waddle, J.A., and Seydoux, G. (2000). Asymmetric segregation of PIE-1 in C. elegans is mediated by two complementary mechanisms that act through separate PIE-1 protein domains. Mol Cell *6*, 445-455.
Soloviev, A., Gallagher, J., Marnef, A., and Kuwabara, P.E. (2011). C. elegans patched-3 is an essential gene implicated in osmoregulation and requiring an intact permease transporter domain. Dev Biol *351*, 242-253.
Sugawara, K., Morita, K., Ueno, N., and Shibuya, H. (2001). BIP, a BRAM-interacting protein involved in TGF-beta signalling, regulates body length in Caenorhabditis elegans. Genes Cells *6*, 599-606.
Thacker, C., and Rose, A.M. (2000). A look at the Caenorhabditis elegans Kex2/Subtilisin-like proprotein convertase family. Bioessays *22*, 545-553.

Wang, L., Eckmann, C.R., Kadyk, L.C., Wickens, M., and Kimble, J. (2002). A regulatory cytoplasmic poly(A) polymerase in Caenorhabditis elegans. Nature *419*, 312-316.
Yokoyama, K., Fukumoto, K., Murakami, T., Harada, S., Hosono, R., Wadhwa, R., Mitsui, Y., and Ohkuma, S. (2002). Extended longevity of Caenorhabditis elegans by knocking in extra copies of hsp70F, a homolog of mot-2 (mortalin)/mthsp70/Grp75. FEBS Lett *516*, 53-57.
Yoneda, T., Benedetti, C., Urano, F., Clark, S.G., Harding, H.P., and Ron, D. (2004). Compartment-specific perturbation of protein handling activates genes encoding mitochondrial chaperones. J Cell Sci *117*, 4055-4066.

References associated with Table S4: *C. elegans* and bacterial strains used in this study.

Alper, S., McElwee, M.K., Apfeld, J., Lackford, B., Freedman, J.H., and Schwartz, D.A. (2010). The Caenorhabditis elegans germ line regulates distinct signaling pathways to control lifespan and innate immunity. J Biol Chem *285*, 1822-1828.
Bolz, D.D., Tenor, J.L., and Aballay, A. (2010). A conserved PMK-1/p38 MAPK is required in caenorhabditis elegans tissue-specific immune response to Yersinia pestis infection. J Biol Chem *285*, 10832-10840.
Brenner, S. (1974). The genetics of Caenorhabditis elegans. Genetics *77*, 71-94.
Calfon, M., Zeng, H., Urano, F., Till, J.H., Hubbard, S.R., Harding, H.P., Clark, S.G., and Ron, D. (2002). IRE1 couples endoplasmic reticulum load to secretory capacity by processing the XBP-1 mRNA. Nature *415*, 92-96.
Chalfie, M., and Sulston, J. (1981). Developmental genetics of the mechanosensory neurons of Caenorhabditis elegans. Dev Biol *82*, 358-370.
Couillault, C., Pujol, N., Reboul, J., Sabatier, L., Guichou, J.F., Kohara, Y., and Ewbank, J.J. (2004). TLR-independent control of innate immunity in Caenorhabditis elegans by the TIR domain adaptor protein TIR-1, an ortholog of human SARM. Nat Immunol *5*, 488-494.
Dworkin, J., and Losick, R. (2005). Developmental commitment in a bacterium. Cell *121*, 401-409.
Estes, K.A., Dunbar, T.L., Powell, J.R., Ausubel, F.M., and Troemel, E.R. (2010). bZIP transcription factor zip-2 mediates an early response to Pseudomonas aeruginosa infection in Caenorhabditis elegans. Proc Natl Acad Sci U S A *107*, 2153-2158.
Fire, A., Xu, S., Montgomery, M.K., Kostas, S.A., Driver, S.E., and Mello, C.C. (1998). Potent and specific genetic interference by double-stranded RNA in Caenorhabditis elegans. Nature *391*, 806-811.
Gray, J.M., Karow, D.S., Lu, H., Chang, A.J., Chang, J.S., Ellis, R.E., Marletta, M.A., and Bargmann, C.I. (2004). Oxygen sensation and social feeding mediated by a C. elegans guanylate cyclase homologue. Nature *430*, 317-322.
Hong, K., Mano, I., and Driscoll, M. (2000). In vivo structure-function analyses of Caenorhabditis elegans MEC-4, a candidate mechanosensory ion channel subunit. J Neurosci *20*, 2575-2588.
Hope, I.A. (1999). C. elegans: A practical approach (Oxford University Press).
Irazoqui, J.E., Troemel, E.R., Feinbaum, R.L., Luhachack, L.G., Cezairliyan, B.O., and Ausubel, F.M. (2010). Distinct pathogenesis and host responses during infection of C. elegans by P. aeruginosa and S. aureus. PLoS Pathog *6*, e1000982.
Iser, W.B., Wilson, M.A., Wood, W.H., 3rd, Becker, K., and Wolkow, C.A. (2011). Co-regulation of the DAF-16 target gene, cyp-35B1/dod-13, by HSF-1 in C. elegans dauer larvae and daf-2 insulin pathway mutants. PLoS One *6*, e17369.

Jose, A.M., Smith, J.J., and Hunter, C.P. (2009). Export of RNA silencing from C. elegans tissues does not require the RNA channel SID-1. Proc Natl Acad Sci U S A *106*, 2283-2288.
Kamath, R.S., Fraser, A.G., Dong, Y., Poulin, G., Durbin, R., Gotta, M., Kanapin, A., Le Bot, N., Moreno, S., Sohrmann, M.*, et al.* (2003). Systematic functional analysis of the Caenorhabditis elegans genome using RNAi. Nature *421*, 231-237.
Kim, D.H., Feinbaum, R., Alloing, G., Emerson, F.E., Garsin, D.A., Inoue, H., Tanaka-Hino, M., Hisamoto, N., Matsumoto, K., Tan, M.W.*, et al.* (2002). A conserved p38 MAP kinase pathway in Caenorhabditis elegans innate immunity. Science *297*, 623-626.
Lamitina, T., Huang, C.G., and Strange, K. (2006). Genome-wide RNAi screening identifies protein damage as a regulator of osmoprotective gene expression. Proc Natl Acad Sci U S A *103*, 12173-12178.
Lewis, J.A., and Hodgkin, J.A. (1977). Specific neuroanatomical changes in chemosensory mutants of the nematode Caenorhabditis elegans. J Comp Neurol *172*, 489-510.
Libina, N., Berman, J.R., and Kenyon, C. (2003). Tissue-specific activities of C. elegans DAF-16 in the regulation of lifespan. Cell *115*, 489-502.
Link, C.D., and Johnson, C.J. (2002). Reporter transgenes for study of oxidant stress in Caenorhabditis elegans. Methods Enzymol *353*, 497-505.
McEwan, D.L., Kirienko, N.V., and Ausubel, F.M. (2012). Pseudomonas aeruginosa Exotoxin A Triggers an Immune Response in Caenorhabditis elegans through Translational Inhibition. Cell Host Microbe *IN PRESS*.
Mizuno, T., Hisamoto, N., Terada, T., Kondo, T., Adachi, M., Nishida, E., Kim, D.H., Ausubel, F.M., and Matsumoto, K. (2004). The Caenorhabditis elegans MAPK phosphatase VHP-1 mediates a novel JNK-like signaling pathway in stress response. EMBO J *23*, 2226-2234.
Powell, J.R., Kim, D.H., and Ausubel, F.M. (2009). The G protein-coupled receptor FSHR-1 is required for the Caenorhabditis elegans innate immune response. Proc Natl Acad Sci U S A *106*, 2782-2787.
Prahlad, V., Cornelius, T., and Morimoto, R.I. (2008). Regulation of the cellular heat shock response in Caenorhabditis elegans by thermosensory neurons. Science *320*, 811-814.
Pujol, N., Zugasti, O., Wong, D., Couillault, C., Kurz, C.L., Schulenburg, H., and Ewbank, J.J. (2008). Anti-fungal innate immunity in C. elegans is enhanced by evolutionary diversification of antimicrobial peptides. PLoS Pathog *4*, e1000105.
Rual, J.F., Ceron, J., Koreth, J., Hao, T., Nicot, A.S., Hirozane-Kishikawa, T., Vandenhaute, J., Orkin, S.H., Hill, D.E., van den Heuvel, S.*, et al.* (2004). Toward improving Caenorhabditis elegans phenome mapping with an ORFeome-based RNAi library. Genome Res *14*, 2162-2168.
Shivers, R.P., Kooistra, T., Chu, S.W., Pagano, D.J., and Kim, D.H. (2009). Tissue-specific activities of an immune signaling module regulate physiological responses to pathogenic and nutritional bacteria in C. elegans. Cell Host Microbe *6*, 321-330.
Shivers, R.P., Pagano, D.J., Kooistra, T., Richardson, C.E., Reddy, K.C., Whitney, J.K., Kamanzi, O., Matsumoto, K., Hisamoto, N., and Kim, D.H. (2010). Phosphorylation of the conserved transcription factor ATF-7 by PMK-1 p38 MAPK regulates innate immunity in Caenorhabditis elegans. PLoS Genet *6*, e1000892.
Shtonda, B.B., and Avery, L. (2006). Dietary choice behavior in Caenorhabditis elegans. J Exp Biol *209*, 89-102.
Sieburth, D., Ch'ng, Q., Dybbs, M., Tavazoie, M., Kennedy, S., Wang, D., Dupuy, D., Rual, J.F., Hill, D.E., Vidal, M.*, et al.* (2005). Systematic analysis of genes required for synapse structure and function. Nature *436*, 510-517.

Smith, P., Leung-Chiu, W.M., Montgomery, R., Orsborn, A., Kuznicki, K., Gressman-Coberly, E., Mutapcic, L., and Bennett, K. (2002). The GLH proteins, Caenorhabditis elegans P granule components, associate with CSN-5 and KGB-1, proteins necessary for fertility, and with ZYX-1, a predicted cytoskeletal protein. Dev Biol *251*, 333-347.
Sze, J.Y., Victor, M., Loer, C., Shi, Y., and Ruvkun, G. (2000). Food and metabolic signalling defects in a Caenorhabditis elegans serotonin-synthesis mutant. Nature *403*, 560-564.
Tabara, H., Sarkissian, M., Kelly, W.G., Fleenor, J., Grishok, A., Timmons, L., Fire, A., and Mello, C.C. (1999). The rde-1 gene, RNA interference, and transposon silencing in C. elegans. Cell *99*, 123-132.
Winston, W.M., Molodowitch, C., and Hunter, C.P. (2002). Systemic RNAi in C. elegans requires the putative transmembrane protein SID-1. Science *295*, 2456-2459.
Yochem, J., Gu, T., and Han, M. (1998). A new marker for mosaic analysis in Caenorhabditis elegans indicates a fusion between hyp6 and hyp7, two major components of the hypodermis. Genetics *149*, 1323-1334.
Yoneda, T., Benedetti, C., Urano, F., Clark, S.G., Harding, H.P., and Ron, D. (2004). Compartment-specific perturbation of protein handling activates genes encoding mitochondrial chaperones. J Cell Sci *117*, 4055-4066.

References associated with Supplemental Experimental Procedures

Bargmann, C.I., Hartwieg, E., and Horvitz, H.R. (1993). Odorant-selective genes and neurons mediate olfaction in C. elegans. Cell *74*, 515-527.
Hart, A.C. (2006). Behavior. In Wormbook, A.C. Hart, and V. Ambros, eds. (The C. elegans Research Community).

Supplemental Figure 1

Supplemental Figure 1. Essential gene inactivations stimulate microbial food aversion and development arrest (or delay) phenotypes (relevant to Figure 1)

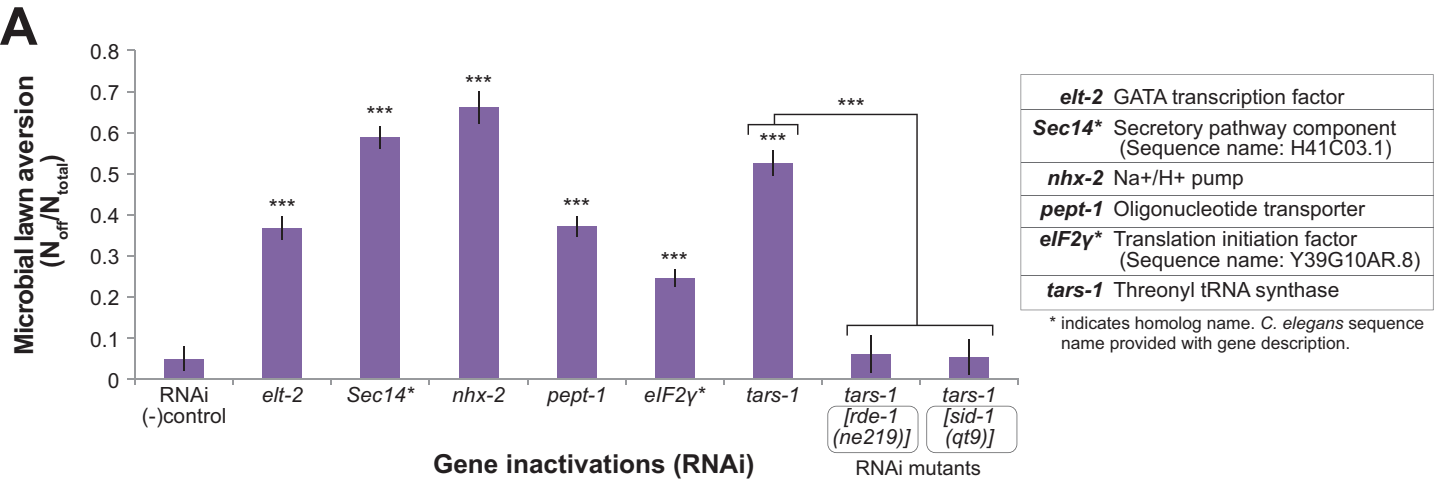

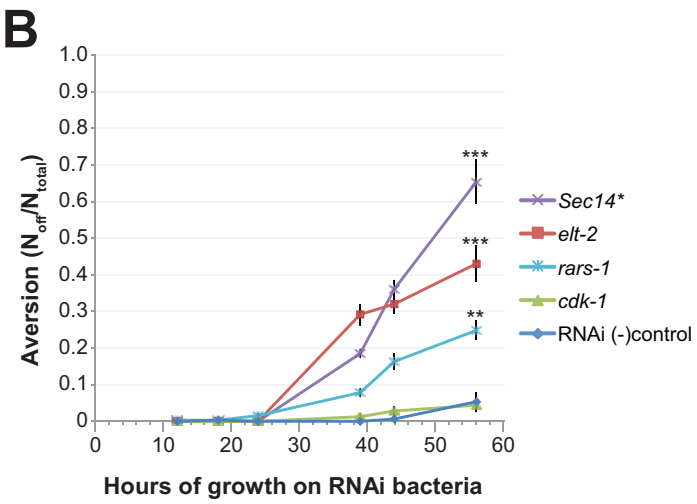

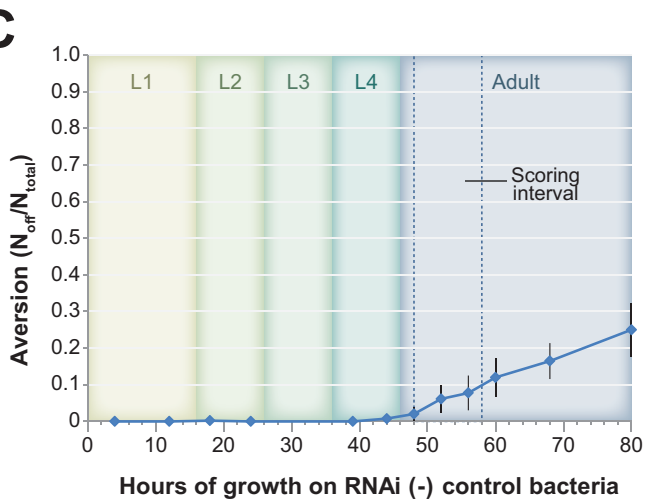

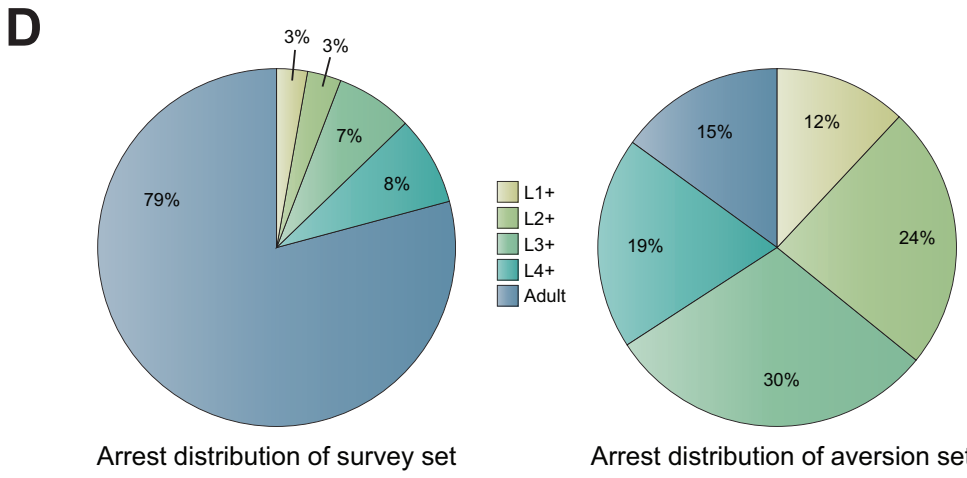

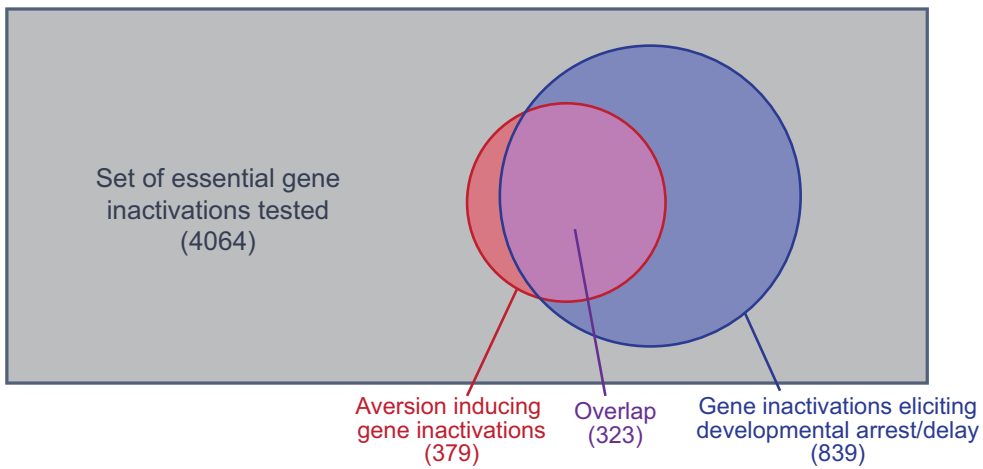

Supplemental Figure 2. Stimulation of pathogen-associated, detoxification, and other transcriptional stress responses by essential gene inactivations (relevant to Figure 3)

A *nlp-29::GFP* (induced by *D. coniospora, S. marcescens* & wounding)

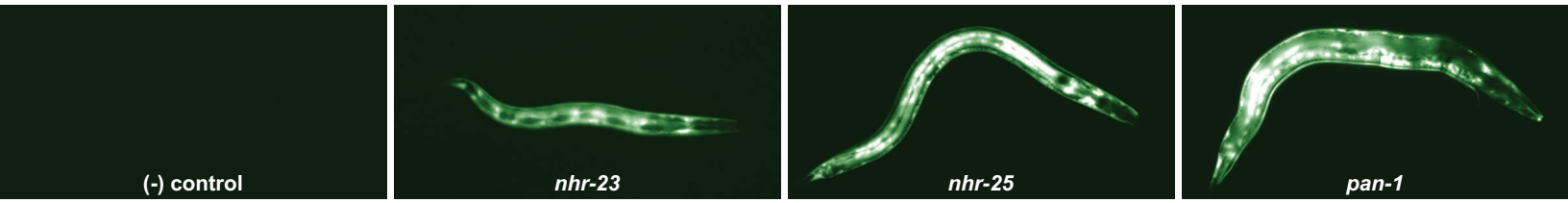

B

gpdh-1::GFP (glyceraldehyde-3-dehydrogenase/osmotic stress reporter)

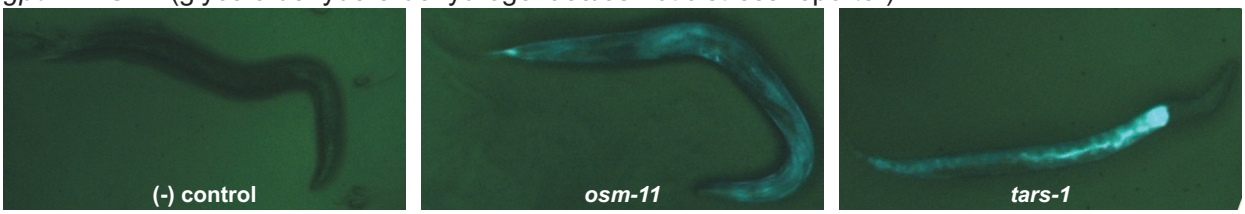

hsp-4::GFP (BiP homolog/ER stress reporter)

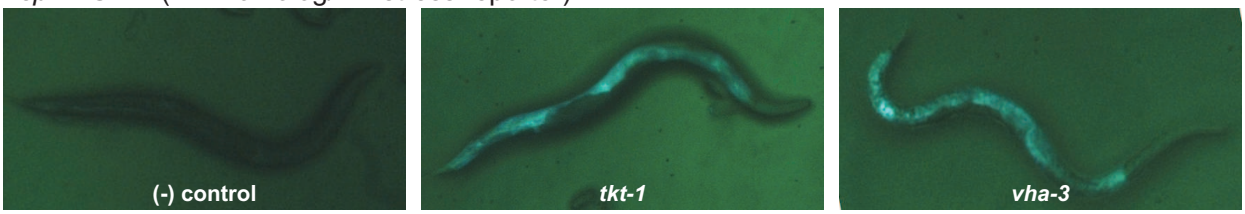

hsp-6::GFP (Hsp70 homolog/mitochondrial stress reporter)

sod-3::GFP (Superoxide dismutase/oxidative stress reporter)

C

GFP reporter	promoter:	Frequency of GFP reporter induction following: RNAi of aversion genes	RNAi of random genes	Fold enrichment
Immune	*clec-60*	59% (n=94)	7% (n=165)	8.0
	irg-1	45% (n=94)	5% (n=165)	9.2
	F35E12.5	24% (n=94)	11% (n=165)	2.2
	nlp-29	28% (n=135)	4% (n=77)	7.2
Detox	*gst-4*	33% (n=83)	5% (n=165)	6.6
	cyp-35B1	40% (n=128)	11% (n=119)	3.6
Other stress	*hsp-6*	43% (n=83)	1.2% (n=146)	34.6
	hsp-4	44% (n=83)	0.0% (n=146)	N/A
	sod-3	32% (n=83)	1.9% (n=146)	17.1
	gdph-1	16% (n=83)	0.6% (n=146)	25.7

p<0.0001 for all aversion vs. random gene set comparisons, chi-squared test

Supplemental Figure 3. Validation and testing of tissue-restricted RNAi strains (relevant to Figure 4)

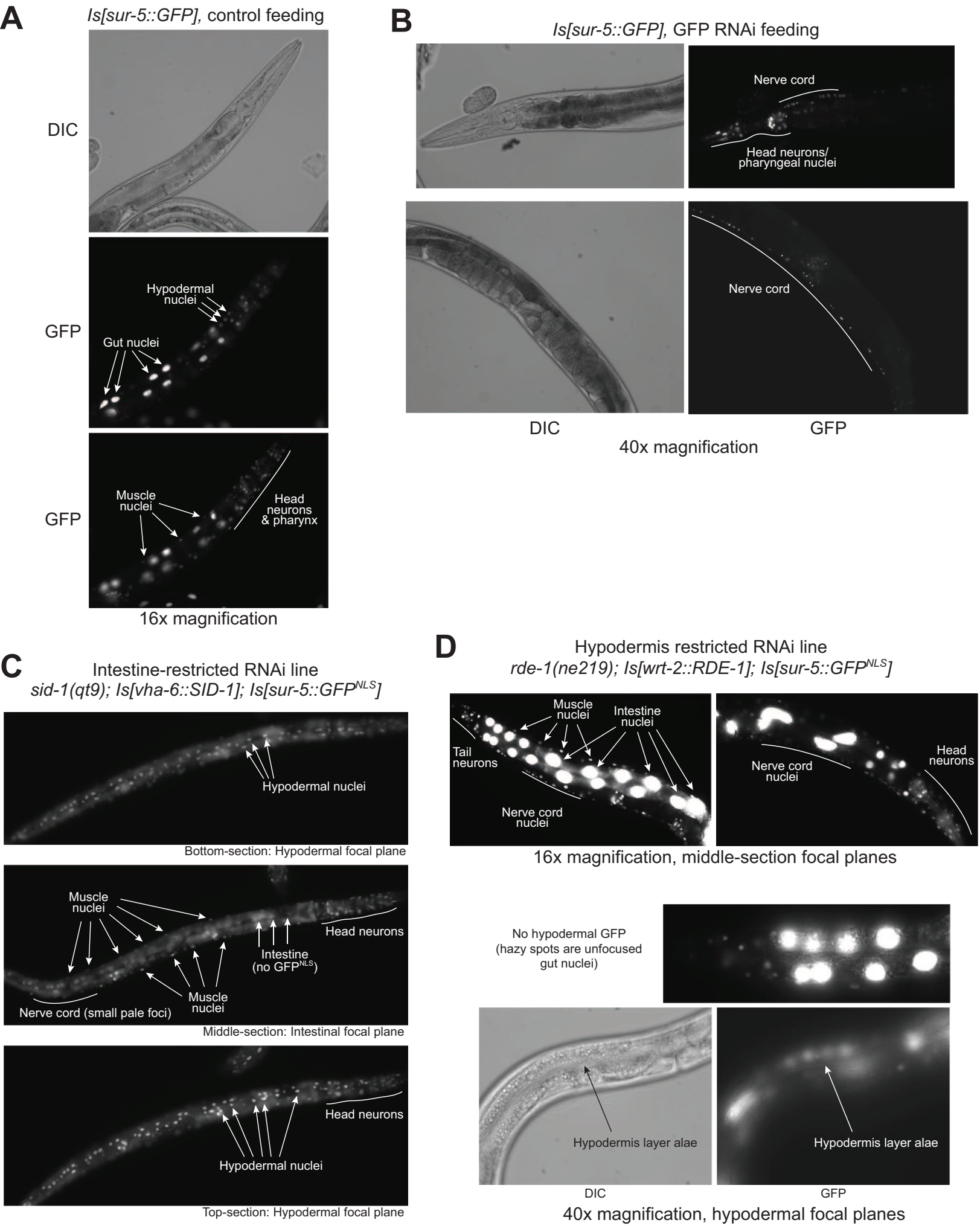

Supplemental Figure 4

Supplemental Figure 4. Tissue-specific gene inactivations (relevant to Figure 4).

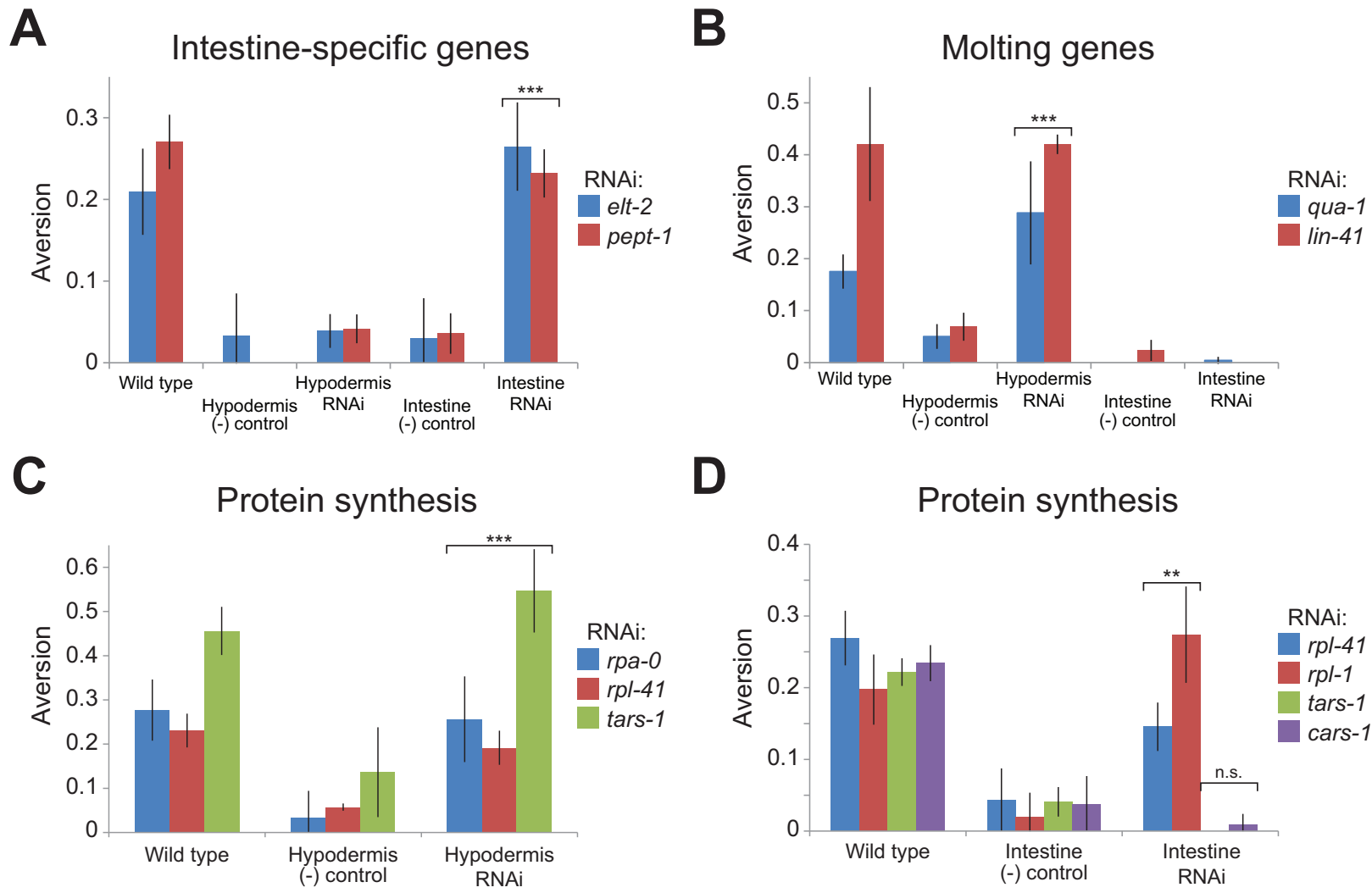

Supplemental Figure 5

Supplemental Figure 5. Analysis of aversion behavior control by known pathogen and stress response pathways (relevant to Figure 5)

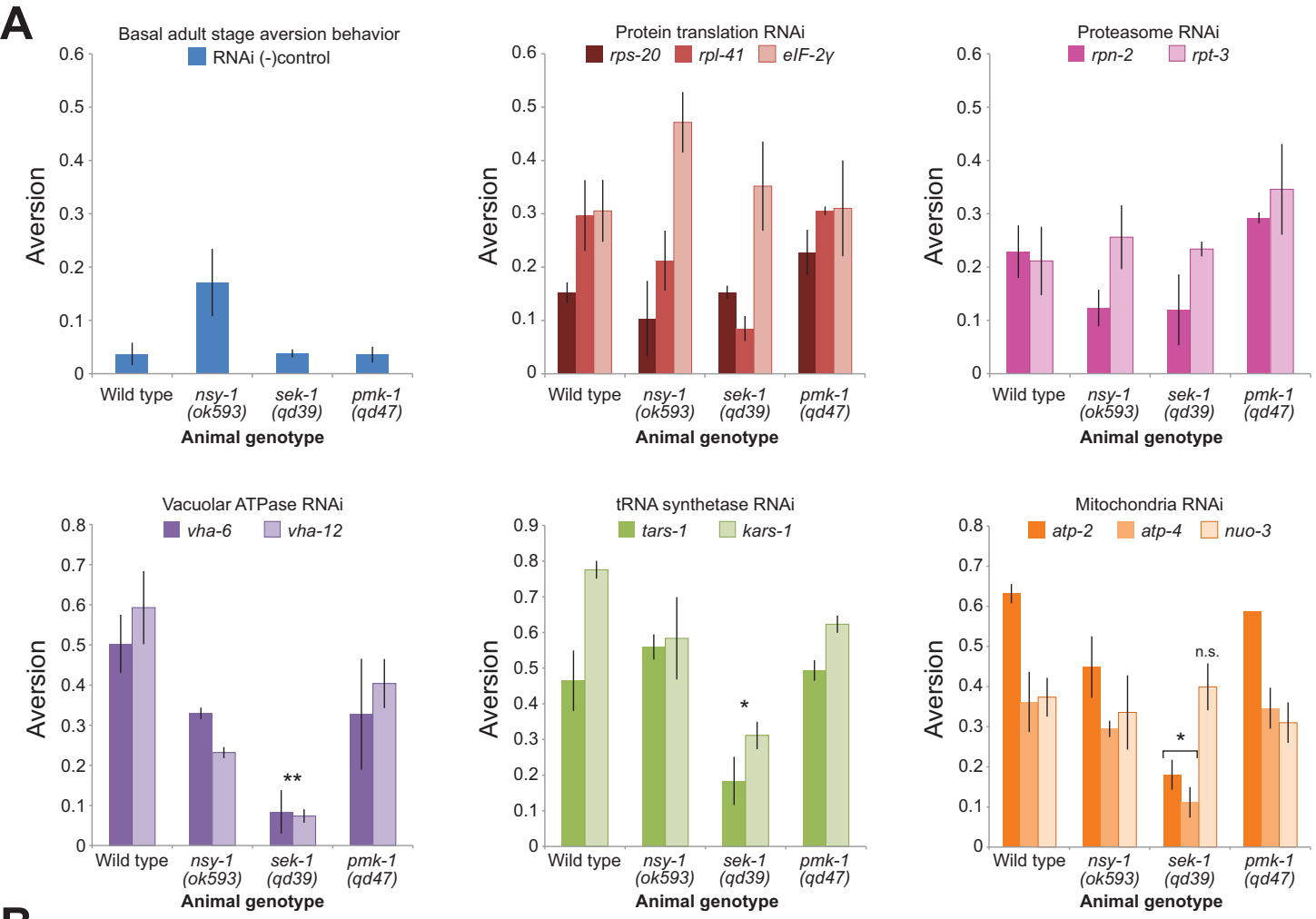

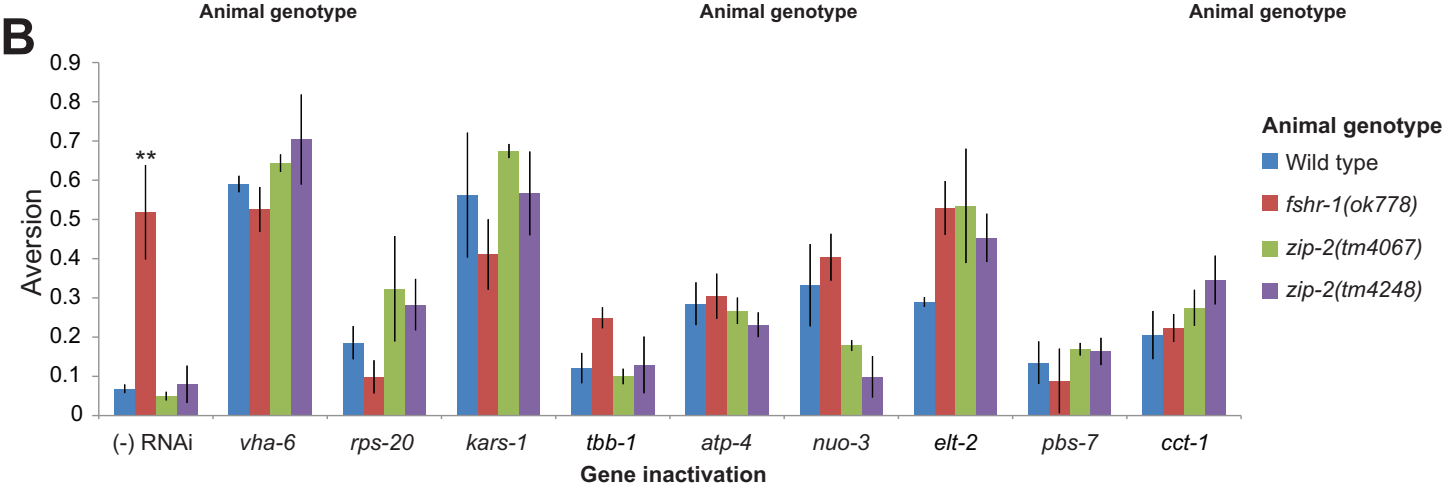

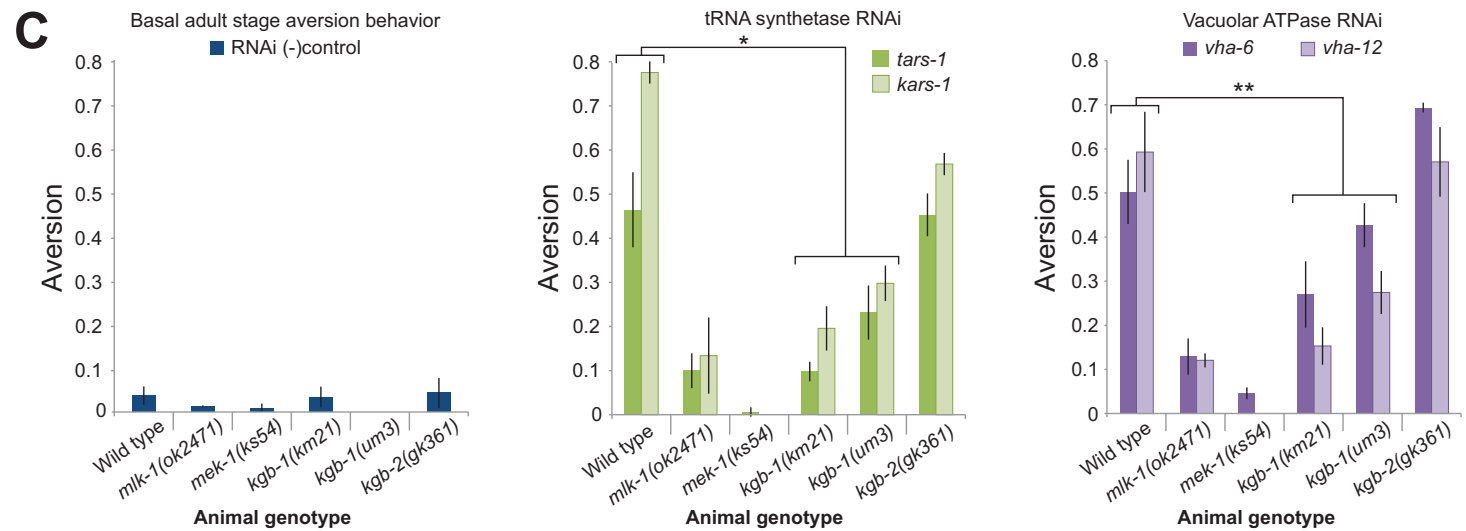

Supplemental Figure 6 Supplemental Figure 6. The function of learning and neurosensation in control of aversion behavior (relevant to Figure 6)

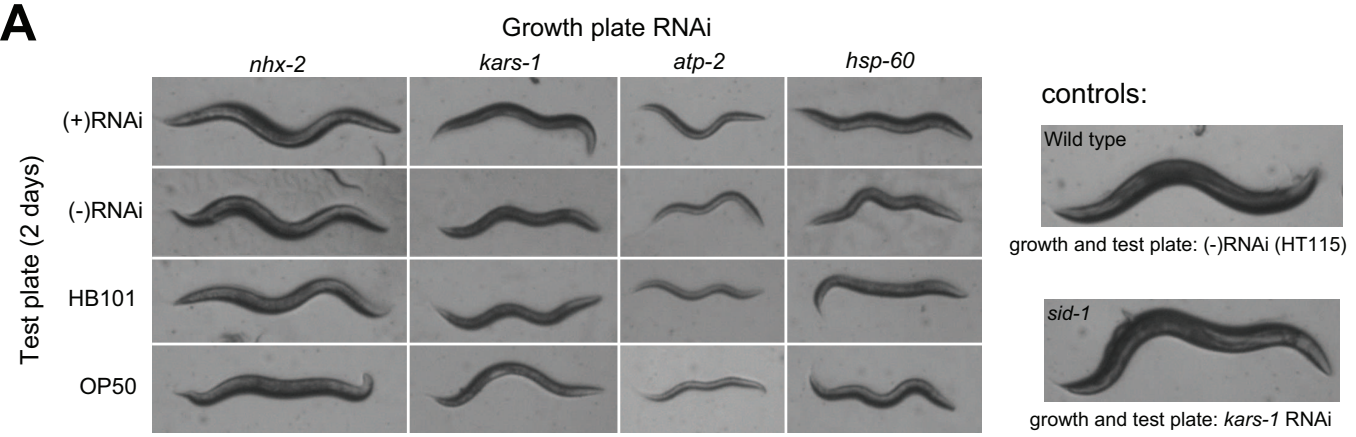

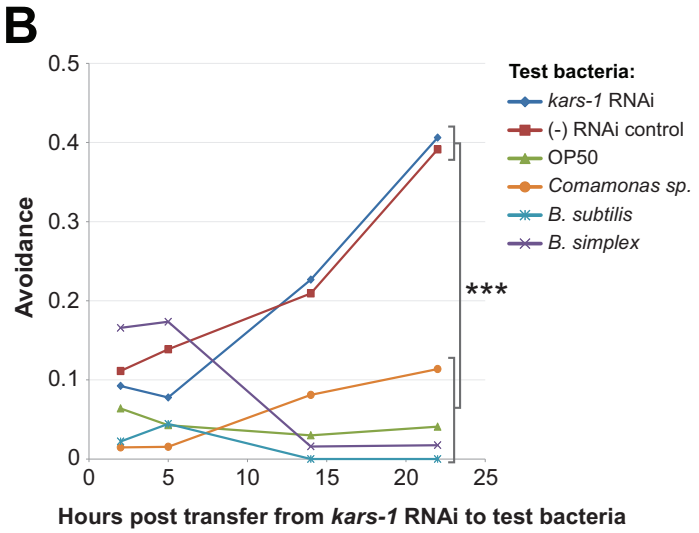

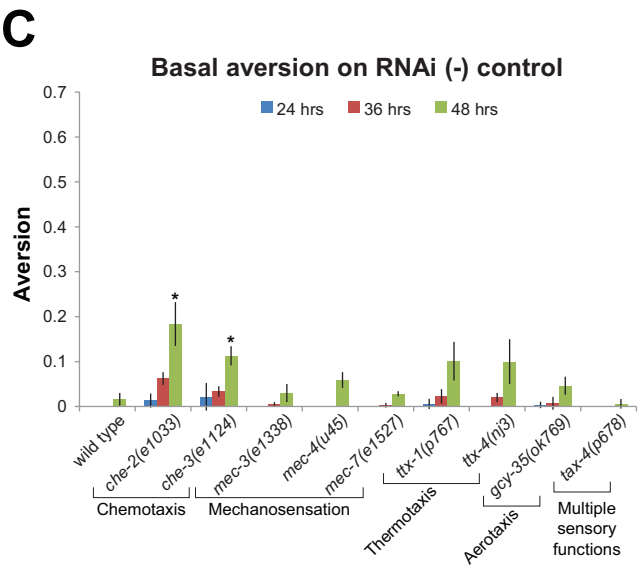

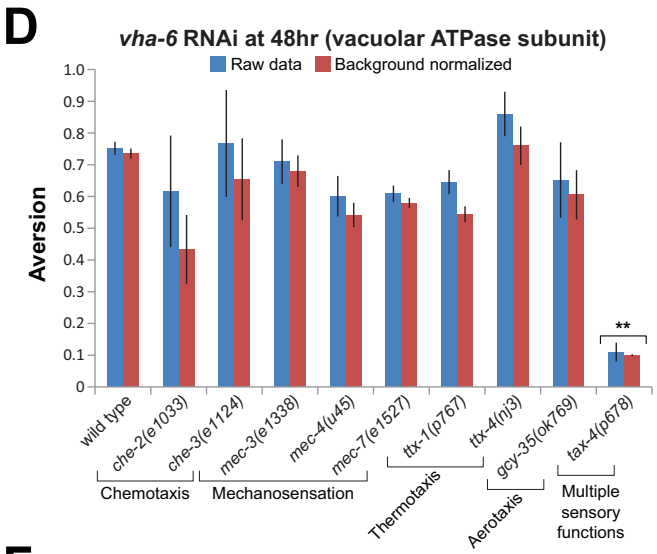

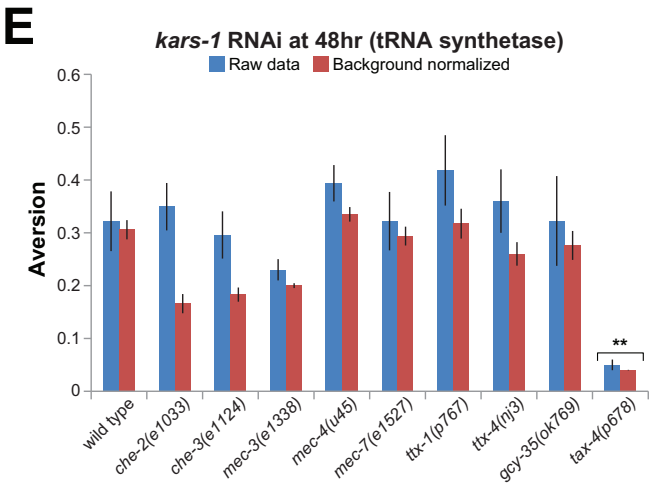

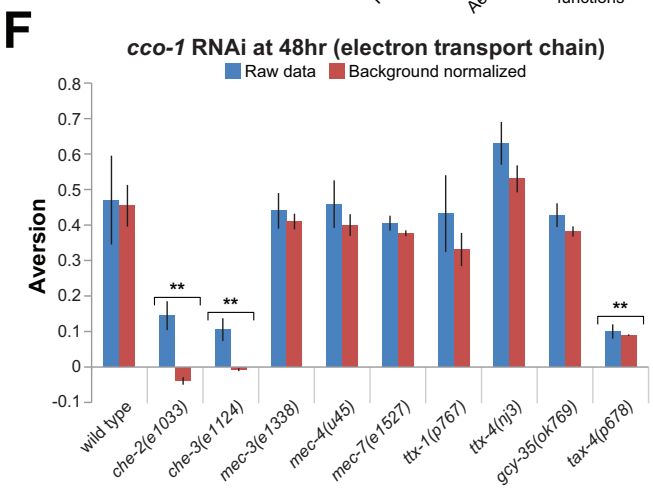

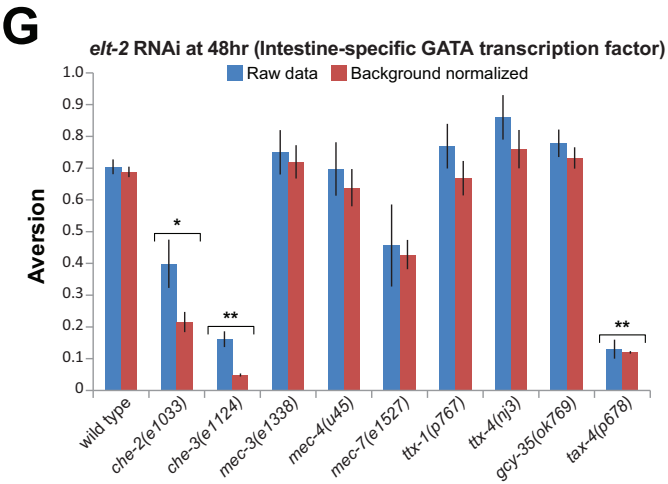

Supplemental Figure 7. Sensory responsiveness of animals in a microbial aversion state induced by essential gene inactivations (relevant to Figure 6)

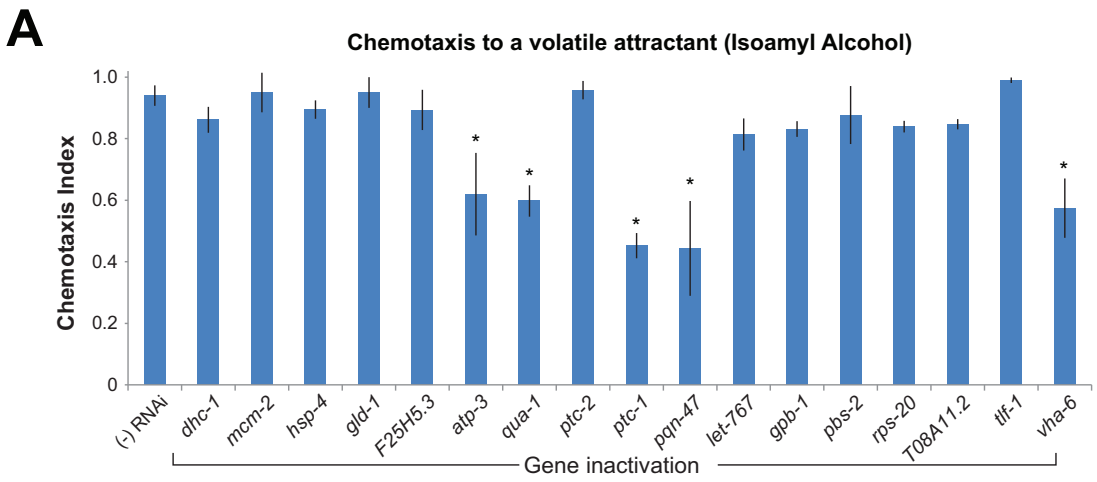

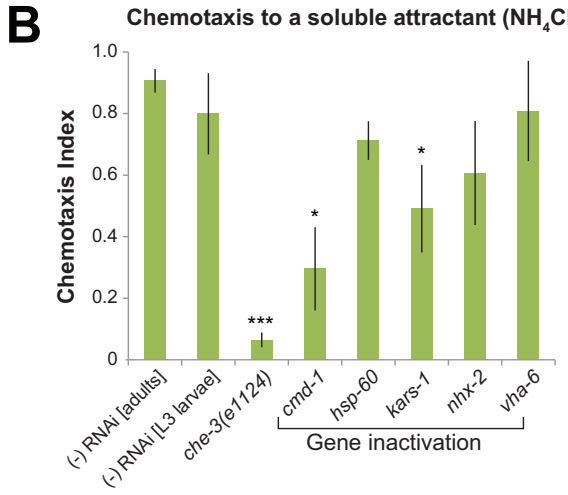

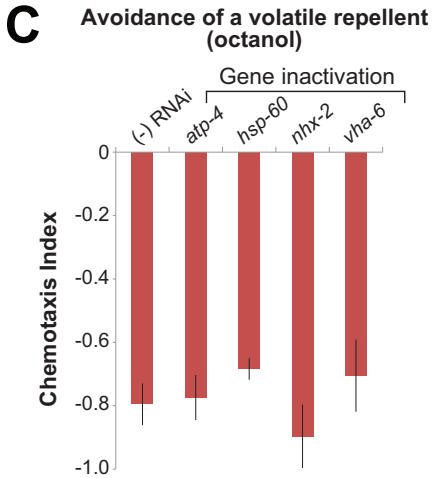

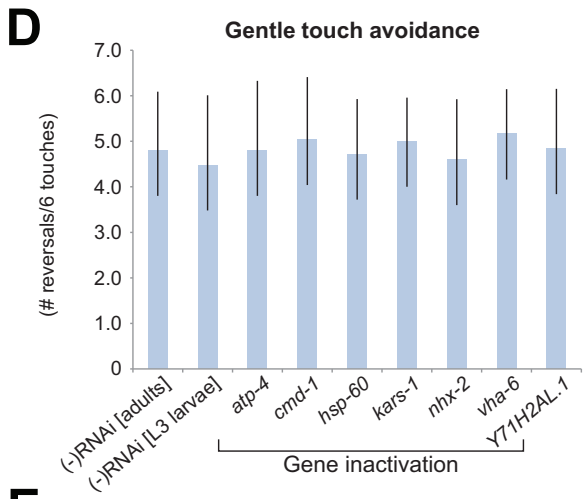

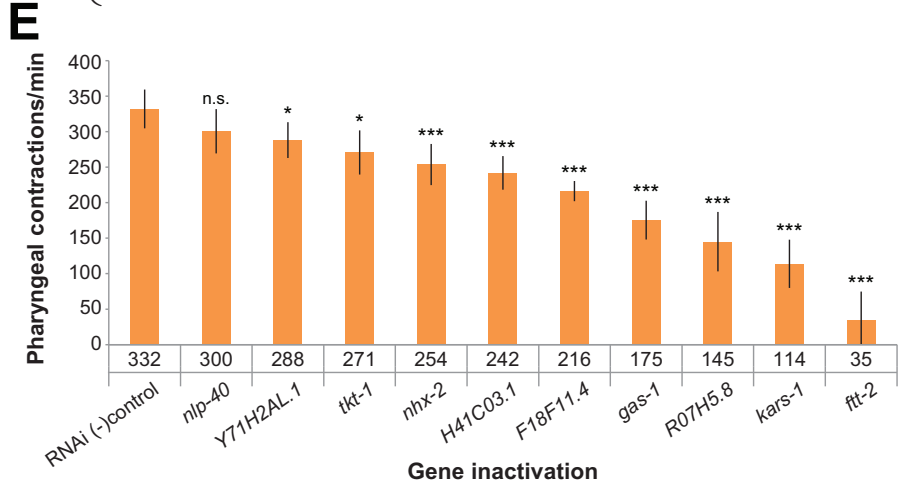

Gene name	Description
nlp-40	Neuropeptide
Y71H2AL.1	Calcineurin B
tkt-1	Transketolase
nhx-2	Na^+/K^+ transporter
H41C03.1	Sec14 homolog
F18F11.4	S/T protein kinase
gas-1	ETC component
R07H5.8	Adenosine kinase
kars-1	tRNA synthetase
ftt-2	14-3-3 protein